Chapter 11
Circularly Polarized Luminescence from Gelator Molecules: From Isolated Molecules to Assemblies

Tonghan Zhao, Pengfei Duan, and Minghua Liu

Abstract Currently, molecular gels have become one kind of the fascinating candidates for fabricating chiroptical materials with circularly polarized luminescence (CPL) properties, due to the tunable and modifiable structure, simple yet facile synthesis, controlled and reversible assembly, and so on. Since self-assembly approach has been regarded as an efficient way for amplifying the chirality, supramolecular gelation provides a remarkable method for fabricating CPL materials with high dissymmetry factor (g_{lum}). Various gel systems, including chiral-, achiral-, organic-inorganic hybrid systems can be endowed with CPL activities through supramolecular gelatinization, possessing excellent luminescence circular polarization. This chapter summarizes and reviews the present status and progress of supramolecular gel systems with CPL activity.

T. Zhao · P. Duan
CAS Center for Excellence in Nanoscience, CAS Key Laboratory of Nanosystem and Hierarchical Fabrication, National Center for Nanoscience and Technology (NCNST), Beijing, P. R. China

University of Chinese Academy of Sciences, Beijing, P. R. China

M. Liu (✉)
CAS Center for Excellence in Nanoscience, CAS Key Laboratory of Nanosystem and Hierarchical Fabrication, National Center for Nanoscience and Technology (NCNST), Beijing, P. R. China

University of Chinese Academy of Sciences, Beijing, P. R. China

Beijing National Laboratory for Molecular Science, CAS Key Laboratory of Colloid, Interface and Chemical Thermodynamics, Institute of Chemistry, Chinese Academy of Sciences, Beijing, P. R. China
e-mail: liumh@iccas.ac.cn

T. Mori (ed.), *Circularly Polarized Luminescence of Isolated Small Organic Molecules*, https://doi.org/10.1007/978-981-15-2309-0_11

11.1 Introduction

Chiroptical materials with circularly polarized luminescence (CPL) activity have been drawing extensive attentions owing to their potential applications in the fields of photoelectric devices [1–3], 3D displays [4], security systems [5], chiral sensing [6–8], asymmetric catalysis [9–13], and so on. In order to get the CPL, it is generally necessary that both the chirality and luminescent chromophore are integrated in one molecule. Thus, various molecules possessing such elements are developed and some typical molecules exhibiting CPL are shown in Fig. 11.1.

It is seen that organic molecules with different kinds of molecular chirality, i.e., point chirality, axial chirality, and planar and helical chirality, can be designed as CPL-active molecules [14–17]. So far, a large number of the organic molecules have been reported to show CPL. In those molecules, the dissymmetry factor defined as $g_{lum} = 2 \times (I_L - I_R)/(I_L + I_R)$, where I_L and I_R are the intensity of left-handed and right-handed circularly polarized light, respectively, is in the range of 10^{-5} to 10^{-3}. Since most of these molecules have been discussed in other chapters, we will not discuss them in detail here.

Among various organic molecules, low-molecular-weight gelator (LMWG) or simply gelator is a unique kind of molecules. The gelator molecules can self-assemble into nanostructures via noncovalent bonds and immobilize certain organic solvents (organogels) or water (hydrogels), as shown in Fig. 11.2. Interestingly, many of the gelator molecules are chiral and some of them show CPL. These gelator molecules have two states, i.e., an isolated molecular state in dilute solution and an assembly state in gels. Interestingly, many of the assembly states showed more intense CPL than that of their isolated molecular state. One of the important directions of CPL research is for materials. Since many materials are in solid or gel state, the research on the CPL of aggregation molecules cannot be avoided. Herein, recent progress in the CPL of the gelator molecules, from isolated molecules to their assembly state, will be discussed.

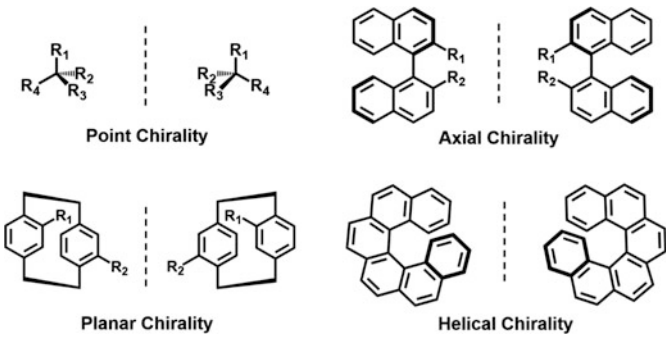

Fig. 11.1 Some typical CPL emitters integrated the chirality and luminescence chromophores. In the case of point chirality, one of the substituent groups is fluorophore

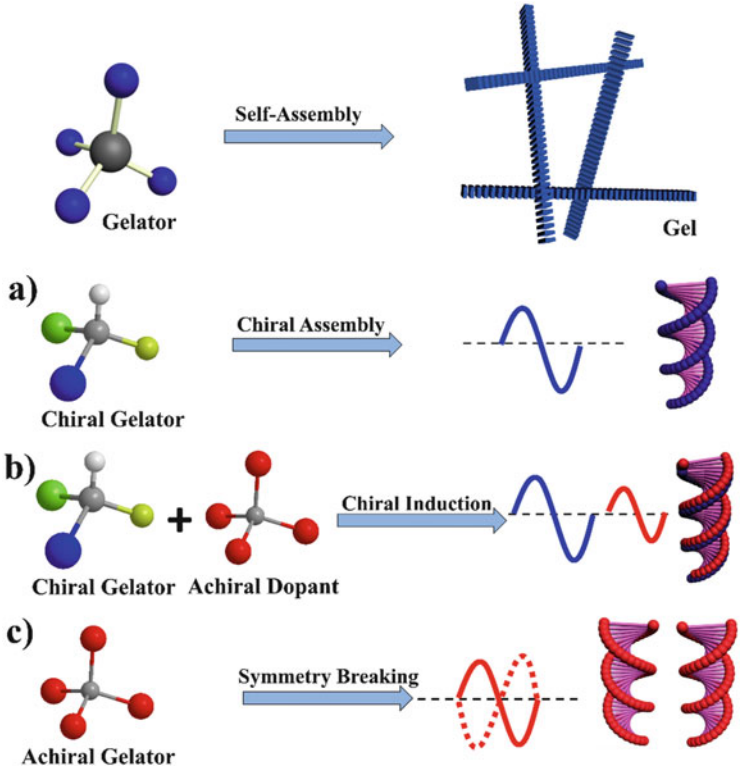

Fig. 11.2 Schematics of gelation induced by self-assembly of gelator (top) and three types of gelation-induced supramolecular chirality (bottom). Chiral gels from (**a**) exclusive chiral gelators, (**b**) the co-assembly of chiral gelator and achiral dopants, and (**c**) exclusive achiral gelators [18]. Copyright 2014, The Royal Society of Chemistry

For the CPL of gelator molecules in a dilute molecular state, it is similar to most of organic molecules. However, in the design of CPL molecules with point chirality, the distance between the chiral center and the chromophore is very important. If the spacer between the chiral center and the chromophore is too long, you cannot get CPL. In the case of CPL from the gelators in assemblies, another phenomenon called aggregation caused quench (ACQ) and aggregation-induced emission (AIE) will frequently appear, which will greatly alter the CPL of the system. These are very important issues which should be considered in the design of the CPL-active gelators.

As illustrated in Fig. 11.2, there are three cases for the design of gelator molecules in order to get the CPL, similar to the formation of the supramolecular chiral gels [18].

The first case is that the isolated gelator shows CPL and the gel showed enhanced or diminished CPL due to the self-assembly. The second case is that the fluorophore does not have any chiral unit. However, when co-assembled with the chiral gelator,

the assemblies showed CPL. In such case, the chiral element is from the nonemissive gelator, while the fluorescence (comes or originates) from the nonchiral fluorophore. The third case is the achiral chromophore without any chiral unit. In molecular state, it does not show any CPL activity. However, upon gelation, symmetry breaking occurs and the CPL could also be obtained.

In this chapter we will start from the design of chiral emissive gelator molecules and then provide the examples of CPL from several typical gelator molecules and their assemblies.

11.2 Design of the Chiral Gelator

The discovery of the gelator was fortuitous in the early stage of the development on supramolecular gels. However, it becomes now possible to design the gelator molecules on purpose. Hinted from the notion of supramolecular synthon in crystal engineering and synthon in organic synthesis, we proposed a concept of gelaton to the design of the gelator [19]. A gelator molecule can be illustrated as in Fig. 11.3.

A gelaton is defined as a special molecule or a structural unit that can be used to formulate the supramolecular gelator and/or gels. Through the covalent bond of the gelaton with certain fluorophore via a linker, it is easier to design the chiral gelator for CPL. Fortunately, many of the gelatons are chiral. Figure 11.3 illustrates several typical gelatons for the design of the gelator molecules, which will be useful for

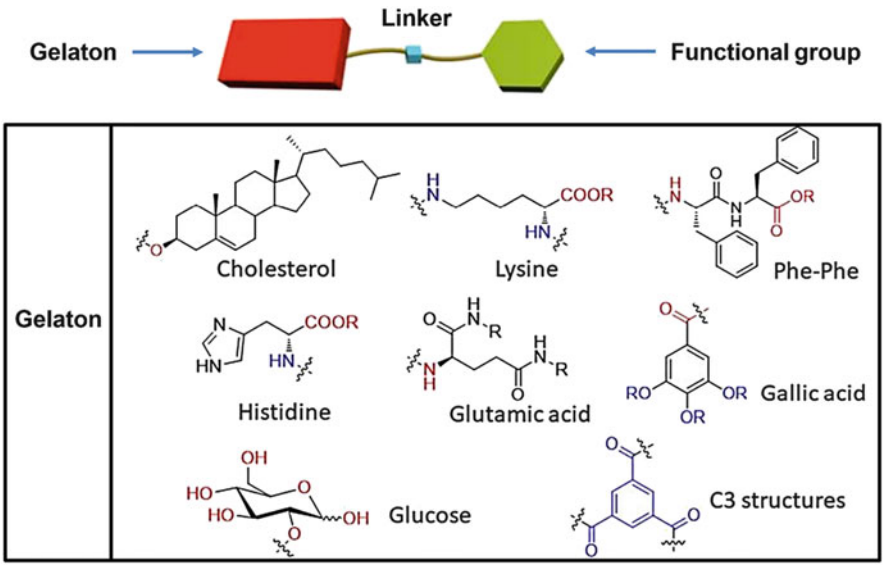

Fig. 11.3 Three main parts of gelator and some typical gelatons [19]. Copyright 2018, The Royal Society of Chemistry

developing various kinds of molecules for CPL research. Among these gelatons, sugar, cholesterol and amino acid derivatives are frequently used. However, only one kind of enantiomers of sugar and cholesterol could be easily obtained, while it is relatively easier to obtain both the *L*- and *D*-enantiomers for amino acids. Thus, CPL-active materials derived from amino acids are extensively investigated.

11.3 CPL from Gelator Molecules and Their Gels

11.3.1 CPL-Active Simple Molecules with Enhanced Circular Polarization via Self-Assembly

For fabricating chiral luminescent molecules, introduction of a luminescent moiety to nonluminous chiral moiety through covalent bond is a general strategy [14]. In this case, lots of chiral moieties bonding with aromatic π-conjugated chromophore exhibited CPL activity have been widely investigated. For example, Kawai and Nakashima et al. reported the CPL from an axial chiral binaphthyl derivatives, in which two perylene bisimides were bonded. The monomeric state in chloroform (molecule **1**, Fig. 11.4a) showed the g_{lum} value as low as 3×10^{-3} [15]. However, the assembly of **1** resulted in almost one order of magnitude higher g_{lum} value. In addition, the morphology of the assemblies played a crucial role in deciding the luminescence dissymmetry. These studies elegantly demonstrated that chiral assemblies could act as an efficient approach to amplify the luminescent dissymmetry factor of simple organic molecules. C_2-symmetrical chiral 1,2-diaminocyclohexane was also used as a chiral source for designing the CPL-active compounds. Strong CPL activity was reported from molecules **2** and **3** (Fig. 11.4b) [20]. For the properties of CPL we could get, the force of the noncovalent interactions, the competition of the chiral and achiral interactions, and the length of fluorophore to the chiral center all have effect. Chiral simple molecules with CPL activity have attracted great interests in recent years and extensive

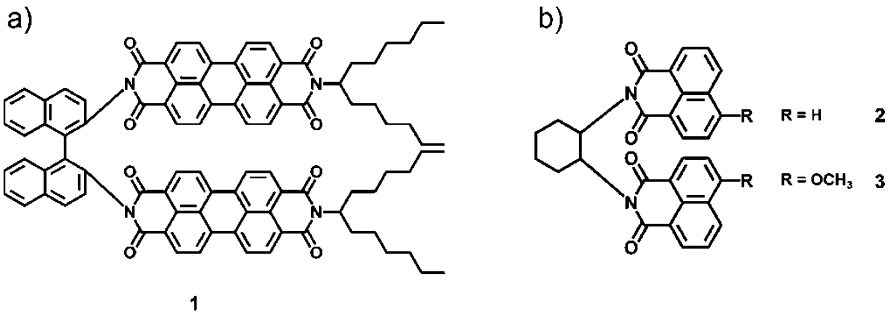

Fig. 11.4 (**a**) Molecular structure of chiral binaphthyl derivatives **1**. (**b**) Molecular structures of chiral diaminocyclohexane derivatives **2** and **3**

accounts and reviews are available; thus, this review will not highlight such a case. We will focus on the recent developments in the field of chiral gelators and chiral supramolecular gels [21].

11.3.2 CPL from Chiral Gelators

11.3.2.1 CPL from Amino Acid Derivative Gelators

In supramolecular gel system, amino acids are excellent gelaton candidates because of its natural chirality, easy accessibility, and wide diversity [19]. For the CPL-active amino acid derivatives, the gelator molecule usually does not show CPL because the spacer between the chromophore and the chiral center is too long. However, upon gelation, the chirality can be transferred to the assemblies which show intense CPL activity. For example, Ihara et al. designed a glutamic acid gelaton-linked anthracene gelator **4** (Fig. 11.5) [22]. Interestingly, no CPL signal was detected for the monomeric state in tetrahydrofuran (THF). However, when **4** formed supramolecular gel through self-assembly in *n*-hexane/THF (50:1), the excimer of anthracene formed and emitted CPL at 25 °C. It was found that the formation of assembly state of **4** could be controlled by temperature. At low temperature,

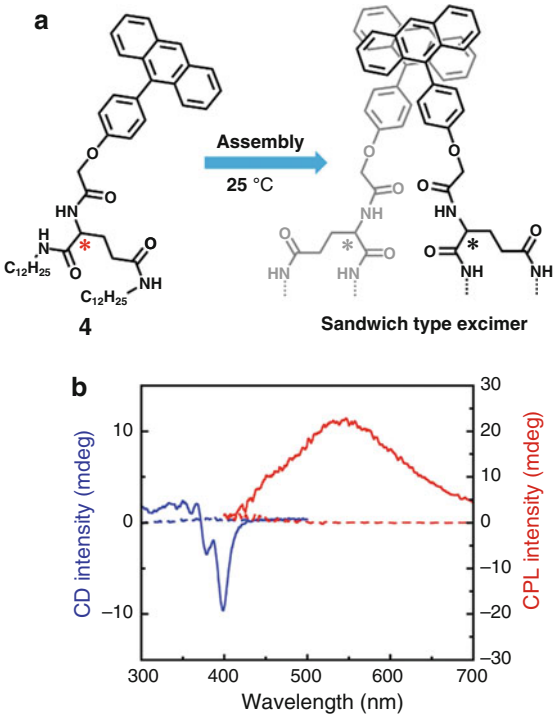

Fig. 11.5 (**a**) Schematic illustration of the excimer formed by molecule **4** in an *n*-hexane/THF (50:1) mixed solution at 25 °C. (**b**) CD (blue line) and CPL (red line) spectra of the **4** gel in an *n*-hexane/THF (50:1) mixed solution (solid line) and in THF (dash line) at 25 °C. Reproduced with permission [22]. Copyright 2015, The Royal Society of Chemistry

intermolecular H-bond was stronger than π–π stacking interaction. Thus, the anthracene chromophores formed twisted stacks with partially overlapped excimer. At 25 °C, the main driving force was π–π stacking for self-assembly. Thus, a Sandwich-type excimer was formed by the anthracene fluorophores in the excited state (Fig. 11.5a). Meanwhile, the obtained gel from gelator **4** with the Sandwich-type excimer can emit intense CPL, with a dissymmetry factor of 3.2×10^{-3} (Fig. 11.5b). In addition, intermolecular interaction became weak at 45 °C; therefore, most anthracene fluorophores could not form an excimer and no CPL could be observed. Therefore, temperature-controlled fluorescence and CPL of organogel was accomplished.

Photon upconversion, in which the higher-energy excited state could be populated by lower-energy light, provides a novel view for achieving higher-energy emission. Duan and Liu et al. proposed an idea to modulate triplet–triplet annihilation-based photon upconversion (TTA-UC) in chiral assembly system, in which they designed a self-assembly system based on anthracene-derived chiral gelator (*L-/D-***5**) as acceptor and achiral Pd^{II} octaethylporphyrin derivative (**6**) as sensitizer [23]. Interestingly, the co-assembly of **6** and *L-/D-***5** via co-gelation could not only generate chirality transfer from *L-/D-***5** to **6**, but also realize triplet–triplet energy transfer (TTET) from **6** to *L-/D-***5**. Thus, dual upconverted (460 nm) and downconverted CPL (550–750 nm) emission was detected in the co-gels under excitation of 532 nm laser (Fig. 11.6a). As shown in Fig. 11.6b, ***L*-5/6** and ***D*-5/6** co-gels in deaerated toluene showed the mirror-imaged upconverted circularly polarized luminescence (UC-CPL) signal at 460 nm. More interestingly, under high excitation laser power, strong CPL signal could be observed in the wide emission range of 550–750 nm (Fig. 11.6c). This strongly suggested that a downconverted CPL could be emitted from **6** in the co-gels at deaerated condition. Thus, a dual circularly polarized light emission involving upconverted CPL at 460 nm and downconverted CPL was realized in co-gels. Two channels of chirality and energy-transfer process were successfully integrated, and the interplay of energy and chirality transfer to produce a dual CPL emission was revealed simultaneously.

Except for glutamic acid-based gelator, an *L*-histidine-derived gelator was designed and the CPL property has been investigated in Fig. 11.7 [24]. As shown in Fig. 11.7a, it was found that a supramolecular gel with CPL properties could be formed by gelator **7** upon sonication. The calculated g_{lum} was $\pm 5.0 \times 10^{-4}$ at 370 nm. In addition, combined with achiral benzoic acids, **7** could form two-component co-gels. Although the benzoic acid is achiral, the co-gels exhibited unexpected enhanced CPL and one order of magnitude amplification of the largest g_{lum} value is detected ($\pm$ 3.0×10^{-3}). The possible mechanism for this CPL enhancement was illustrated in Fig. 11.7b. A bilayer structure could be constructed by gelator **7** due to the H-bond between the imidazole moieties and urea and π–π stacking between the naphthalene. For the co-assembly, a C_3-like secondary unit was firstly formed by **7** and benzoic acid, then this unit further self-assembly into hexagonal structures. The tight π–π interaction in this hexagonal stacking resulted in better chirality transfer from gelator **7** to the supramolecular assembles, which

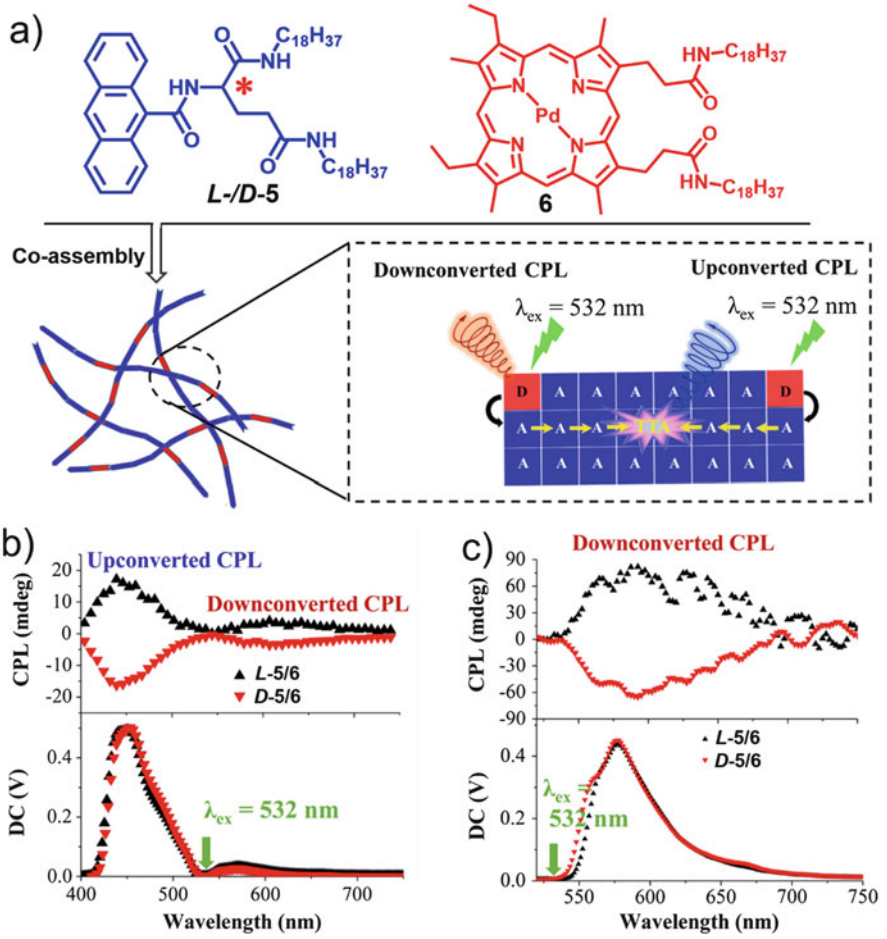

Fig. 11.6 (**a**) Schematics of energy acceptor *L*-**5** or *D*-**5** and energy donor **6** in TTA-UC process. In the co-assembly system, the chirality can be transferred from gel **5** to **6**. (**b**) CPL spectra of *L*-**5/6** and *D*-**5/6** in deaerated toluene, $\lambda_{ex} = 532$ nm laser. (**c**) CPL spectra of *L*-**5/6** and *D*-**5/6** in deaerated toluene, $\lambda_{ex} = 532$ nm laser. Reproduced with permission [23]. Copyright 2018, WILEY-VCH

might further profit the $(I_L - I_R)$ values. In addition, the total fluorescence intensity $(I_L + I_R)$ decreased after adding benzoic acid. Based on the $g_{lum} = 2 \times (I_L - I_R)/(I_L + I_R)$, an amplification of the CPL resulted from lower $(I_L + I_R)$ values could be observed.

11.3.2.2 Aggregation-Induced Emission (AIE) Triggered CPL in Gels

As stated above, the regulated assembly of chiral emitters would be one of the general and simple ways adopted for enhancing g_{lum}. However, due to the aggregation-caused quenching (ACQ) effect, which leads to a much lower or

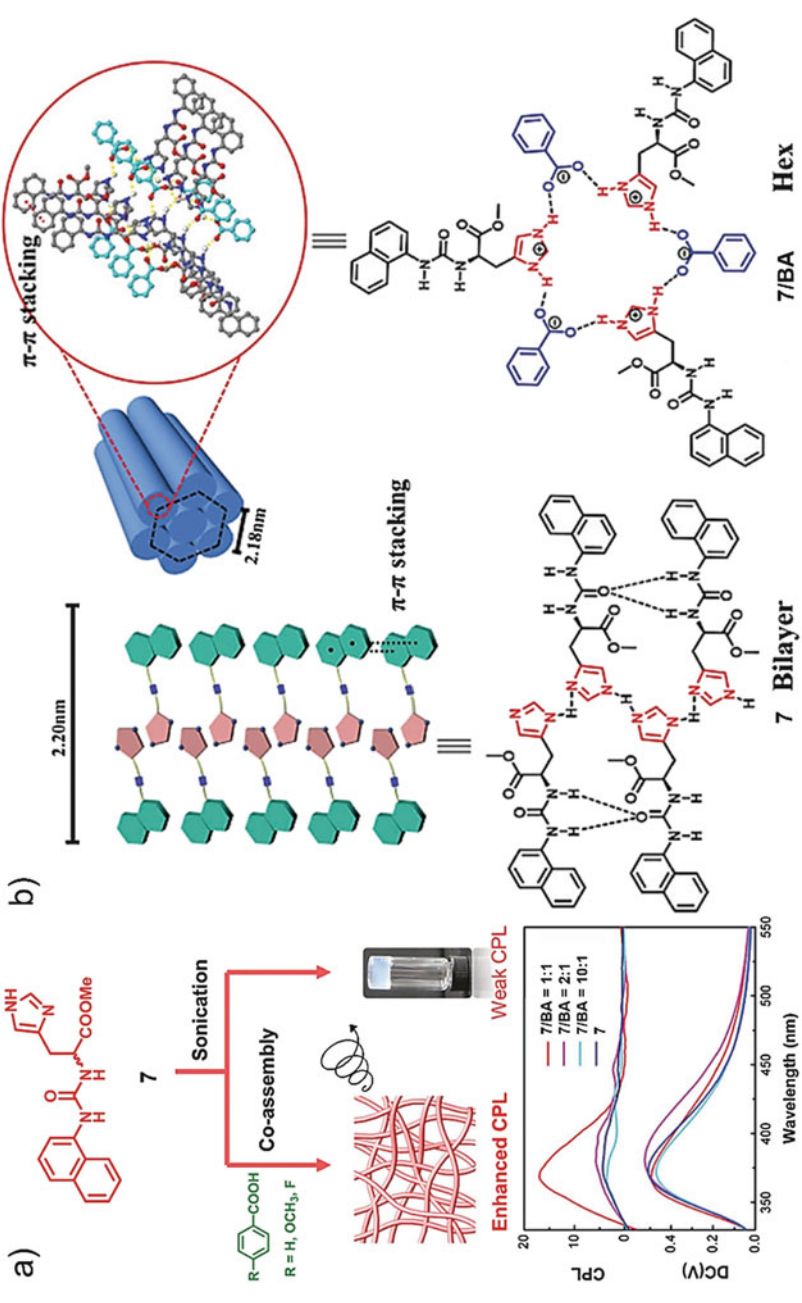

Fig. 11.7 (**a**) Schematics of the achiral molecule-boosted CPL in histidine-derived naphthalene organogels (up) and CPL spectra of **7** (gel) and co-assemblies of **7** with BA in different ratios (bottom). (**b**) Schematic illustration of the molecule packing modes of **7** self-assemblies and the **7**/BA co-assemblies. Reproduced with permission [24]. Copyright 2018, The Royal Society of Chemistry

even no emission performance of luminophores in the aggregated state, the CPL performance of most luminophores becomes even worse from isolate molecule to aggregated state. Fortunately, Tang's group advanced an excellent idea to solve this problem by combined aggregation-induced emission (AIE) effect with chiral assembly [25]. AIE luminophore incorporated with the chiral component to fabricate novel CPL-active materials has become an efficient way to achieve both large g_{lum} values and high emission efficiency in condensed phase [26]. Cyano-substituted stilbene (CNSB) is a well-known compound with AIE property. When CNSB conjugated with a glutamic-derived gelaton, an AIE gelator was obtained (*L-/D-***8**) [27]. As shown in Fig. 11.8, the chiral donor (gelator **8**) and achiral acceptor (BPEA) could form a composite nanohelix through co-assembly, in which both energy and chirality transfer were observed simultaneously. Amazingly, not only the chirality transfer happened in the complex, but also the dissymmetry of CPL was significantly amplified during the energy transfer. Thanks to the π–π stacking of CNSB and the H-bond between the amide groups, an ordered nanohelix structure could be obtained from gelator **8** through self-assembly. During the self-assembly process, not only the emission intensity of **8** remarkably increased, but also the molecular level chirality transferred to the supramolecular level, resulting in the excellent CPL properties. When **8** co-assembled with achiral BPEA, the acceptor BPEA was inserted into the nanohelix through the weak π–π stacking to form the co-gel (Fig. 11.8a). Interestingly, the achiral acceptors could be endowed with CPL caused by chirality transfer from the nanohelix. As shown in Fig. 11.8b, the detected CPL g_{lum} value was $\pm 1.2 \times 10^{-3}$ by directly exciting the acceptor (at 400 nm), while the g_{lum} for the acceptor by exciting the donor (at 320 nm) showed a significant enhancement (up to $\pm 3 \times 10^{-3}$). This result exhibited that g_{lum} value of CPL was amplified more than 2.5 times through the energy-transfer process. This might be resulted from the enhancement of acceptor emission via the energy transfer, which seems to further amplify the g_{lum} values.

Encouraged by the result of energy transfer amplified CPL, Liu et al. further investigated a cooperative chirality and sequential energy transfer in a supramolecular co-assembly system to explore its mechanism. In this work, a cyanostilbene-appended glutamate gelator **9** and two kinds of achiral acceptors, thioflavin T (ThT) and acridine orange (AO), were employed to from a co-gel [28]. Similar to gelator **8**, the chiral gelator **9** could form supramolecular nanotubes with CPL activity. In addition, the supramolecular chirality could transfer to these two achiral acceptors through co-assembly. Meantime, the excited-state energy of **9** nanotubes could directly transfer to ThT but only be sequentially transferred to AO. More interestingly, compared with CPL from directly exciting AO, a stepwise amplified CPL could be observed when exciting the donor **9** or intermediate donor ThT in the **9**/ThT/AO ternary system (Fig. 11.9).

It should be noted that energy transfer boosted CPL was considerable, and a possible analysis was proposed. When donor **9** nanotubes are excited by unpolarized light, a CPL is obtained due to its intrinsic chirality. However, when acceptors were added, the excited-state energy with chiral information will transfer to acceptors, resulting in a new CPL from the acceptor. Based on a theoretical

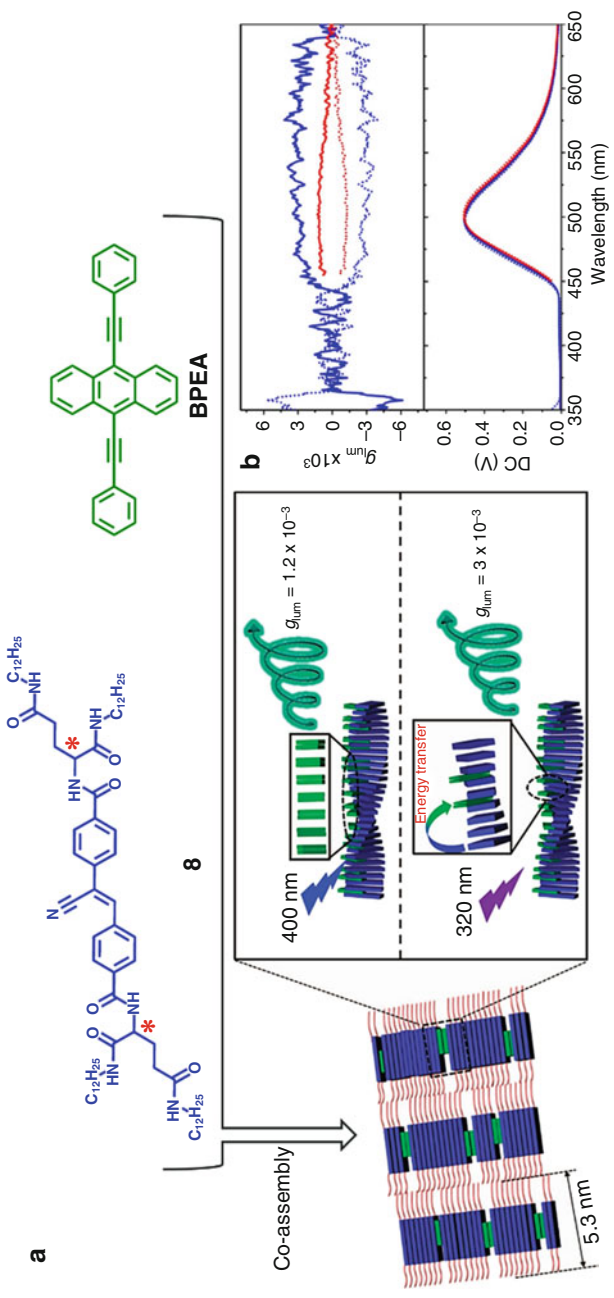

Fig. 11.8 (**a**) Chemical structures of **8** and BPEA, and schematic illustration of energy transfer amplified CPL in co-assembly nanohelix. Under excitation at 400 nm, the composite nanohelix showed green CPL with $g_{lum} = 1.2 \times 10^{-3}$ (top pattern), while energy transfer boosted CPL with a relatively large value $g_{lum} = 3.0 \times 10^{-3}$ under excitation at 320 nm (bottom pattern). (**b**) CPL dissymmetry factor g_{lum} versus wavelength, $\lambda_{ex} = 320$ nm (blue line) and $\lambda_{ex} = 400$ nm (red line). Reproduced with permission [27]. Copyright 2017, Nature Publishing Group

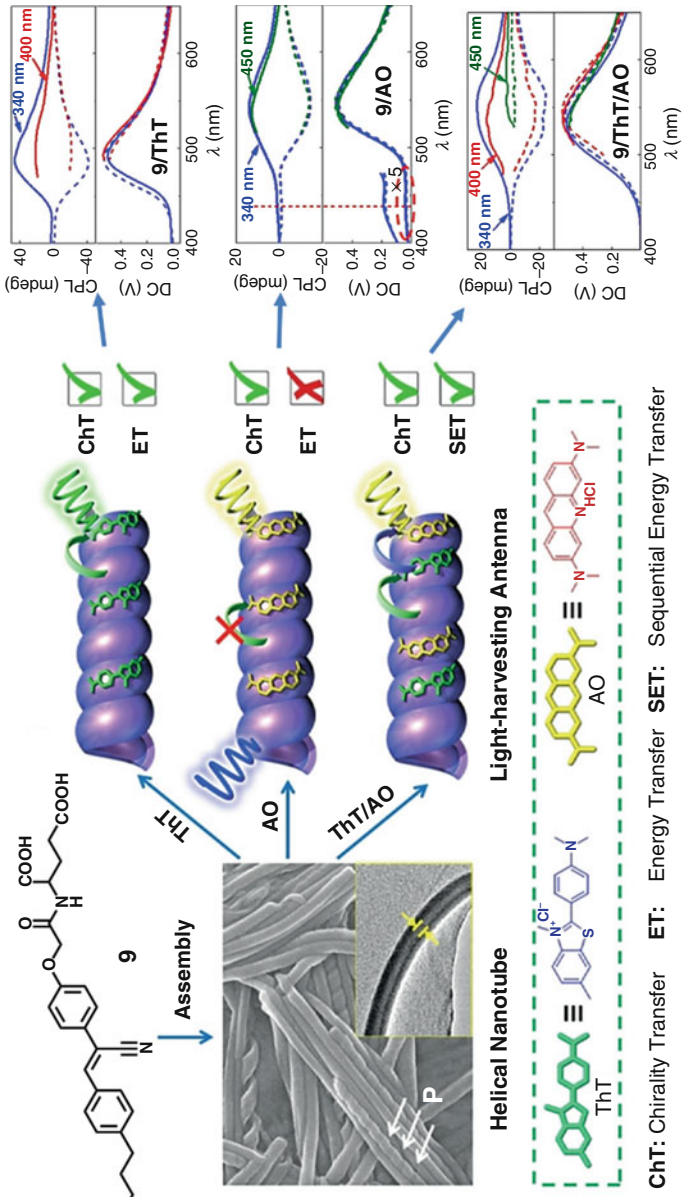

Fig. 11.9 Left: Schematics of the self-assembly **9** nanotubes, and different chirality and energy-transfer modes of the co-assembly of **9**/ThT, **9**/AO, and **9**/ThT/AO. Insets are scanning electron microscopy (SEM) and tunneling electron microscopy (TEM) images of the **9** nanotubes. Right: CPL spectra of **9**/ThT, **9**/AO, and **9**/ThT/AO under different excitation wavelength ($\lambda_{ex} = 340$ nm for **9**, $\lambda_{ex} = 400$ nm for ThT, and $\lambda_{ex} = 450$ nm for AO). Reproduced with permission [28]. Copyright 2019, Wiley-VCH

calculation by Bene and co-workers, in a helicity and energy-transfer process (hFRET), the helicity in fluorescence from a rotating donor dipole could be preserved [29]. In the instance of **9**/ThT/AO system, the helicity of luminescent donor **9** even ThT may be sequentially transferred to acceptor AO and amplified the g_{lum} of AO. For experimental aspect, the *L*-**9**/ThT system exhibited an amplified g_{lum} value (1.89×10^{-2}) when excited by circularly polarized light contrasted to the g_{lum} value excited by unpolarized light ($g_{lum} = 3.3 \times 10^{-3}$). Thus, the helicity in the donor excited state could be transferred to the acceptor and subsequently amplified the g_{lum} was indirectly illustrated.

11.3.2.3 CPL from Chiral π-Conjugated Gelators

In supramolecular gel system, π-conjugated gelators also play an important role because of their unique electronic and optical properties. Ajayaghosh's group has reported the design of oligo(*p*-phenylenevinylene) (OPV)-derived gelators and their hierarchical self-assembly properties [30]. Furthermore, the CPL property of a photosensitive π-conjugated gelator azobenzene-linked phenyleneethynylene (**10**) was also been investigated in Fig. 11.10 [31]. As shown in Fig. 11.10a, the assembly of **10** showed a positive CPL before photoisomerization. Interestingly, the signal of CPL was inverted after irradiation. A possible mechanism for the observed photoinduced CPL inversion resulted from helicity inversion was proposed in Fig. 11.10b. The assembly of **10** groups in methylcyclohexane (MCH) shows *P*-helical. After ultraviolet (UV) photoirradiation, the remaining *E,E* isomers were low in the photostationary state and the excess homonuclear *M*-helical YY aggregates will nucleate and control the self-assembly. Therefore, the photoinduced CPL signal was reversed.

11.3.3 CPL from Achiral Luminophores

11.3.3.1 Symmetry Breaking Triggered CPL

In the above description, luminophores conjugated with chiral gelaton moieties are required for the fabrication of CPL-active gels. Nevertheless, not only chiral gelators but chiral supramolecular gels can be formed by completely achiral gelators through assembly, thus provided the possibility for the exclusive achiral fluorophores to fabricate CPL materials [32]. If an asymmetric environment is provided during self-assembly, some achiral gelators can result spontaneous symmetry breaking to form chiral supramolecular assemblies in this situation. As showed in Fig. 11.11, CPL activities could be observed if an achiral ionic polymer **11** and Rhodamine B were under mechanical stirring [33]. Moreover, the stir direction could determine the CPL signal: a positive sign was resulted from counterclockwise (CCW) stirring, while clockwise (CW) stirring induced a negative sign (Fig. 11.11a). In order to reveal the origin of the CPL, CPL spectra from four different angles of the cuvette

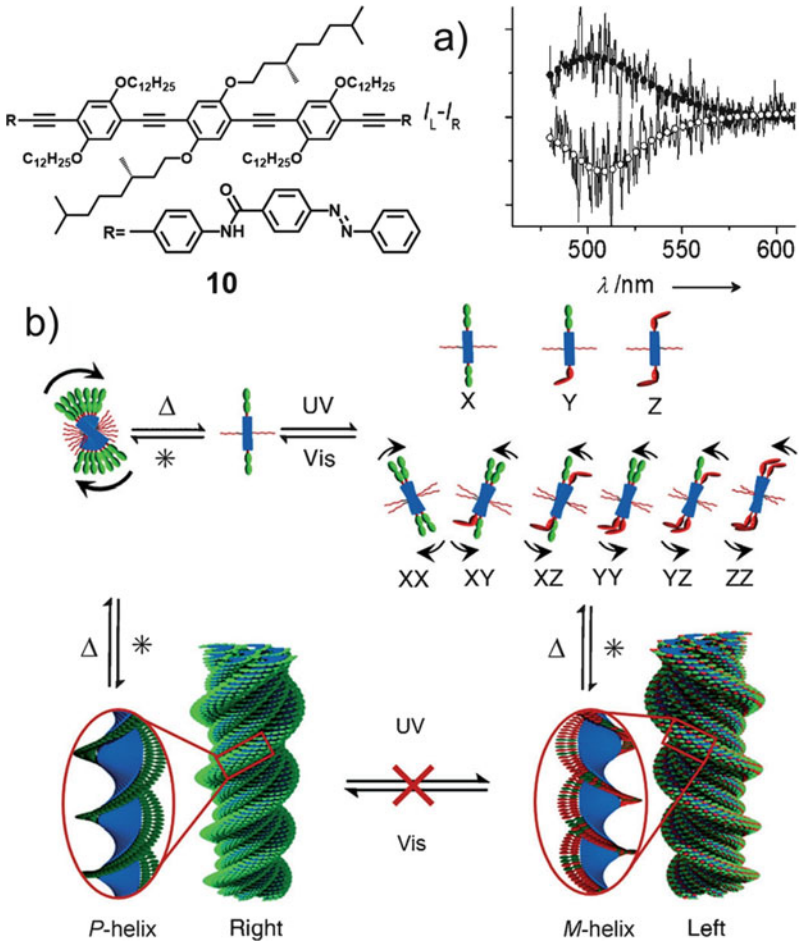

Fig. 11.10 Chemical structure of **10** and (**a**) CPL spectra for **10** before (filled circle) and after (open circle) UV irradiation. (**b**) Schematics of supramolecular helical assembly of **10**'s reversible helicity inversion via a disassembly/reassembly process accompanying with *E/Z* photoisomerization of azobenzene moieties. Δ = heating; ∗ = cooling. Reproduced with permission [31]. Copyright 2012, Wiley-VCH

were detected (Fig. 11.11b). The CPL spectra detected from the four different angles showed a same sign with similar shape in a series of evaluation, indicating that the chirality of Rhodamine B was induced by stir on a macroscopic level. Nevertheless, it should be noted that such CPL only can be observed during the stirring process. Once the stirring stopped, the sample became CPL silent.

In the supramolecular gel systems, an achiral C_3-symmetric gelator was also found to display fascinating CPL performance (Fig. 11.12) [34]. It was found that when the achiral gelators formed the organogels, it showed strong emission as well as the CPL. The handedness of the CPL appeared randomly, suggesting

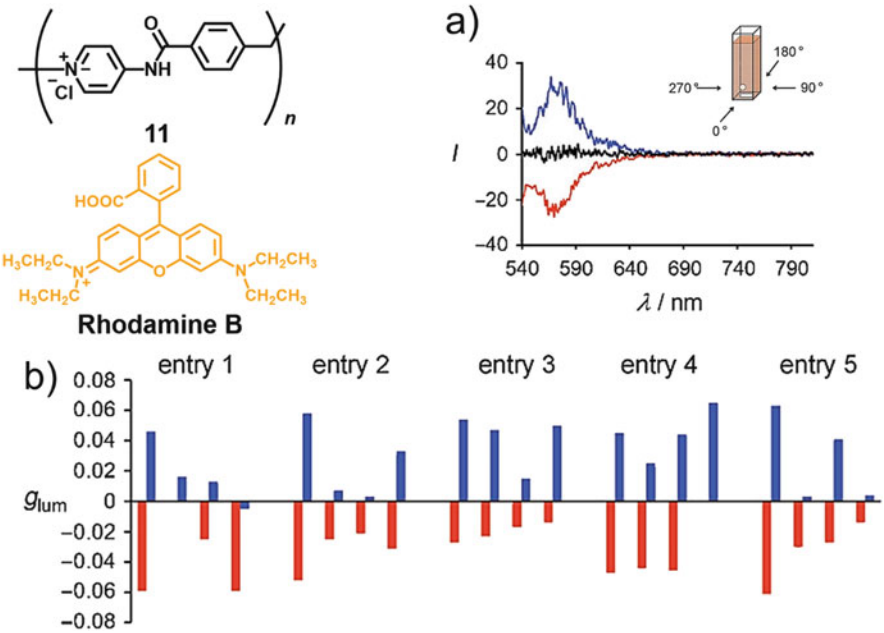

Fig. 11.11 Chemical structures of **11**, Rhodamine B and (**a**) CPL spectra recorded with counter-clockwise (CCW, blue line) stirring, clockwise (CW, red line) stirring, and no stirring (black line). The inset shows the four faces of the cuvette detected for the CPL measurements. (**b**) Statistical distributions of g_{lum} values in five different samples under CCW (blue) and CW (red) stirring preparation in four faces of the sample cuvette. Reproduced with permission [33]. Copyright 2011, Wiley-VCH

a spontaneous symmetry breaking and the g_{lum} value was $\pm 0.8 \times 10^{-2}$, as shown in Fig. 11.12a. Interestingly, in such a system mechanical stirring could enhance the g_{lum} values during the supramolecular gelation process (Fig. 11.12b). In addition, the obtained gel dispersion was quite stable and the CPL remained even after stopping the stirring. However, the direction of the CPL signals could not be controlled by the stirring direction. The direction of CPL signals can be readily regulated by adding some simple chiral dopants (Fig. 11.12c). More interestingly, the g_{lum} value was also amplified by chiral dopants ($\pm$ 2.3 $\times$ 10^{-2}).

In some cases, the CPL from the nanoassemblies based on achiral molecules showed a morphology dependence. As illustrated in Fig. 11.13, twisted ribbons, nanobelts and trumpet-like nanostructures can be formed from an achiral C_3-symmetric molecule via the assembly in a mixed DMF/water solvent [35]. At a unity mixing ratio, nanobelts were observed. Upon increasing the amount of dimethylformamide (DMF), nanotwists and nanotrumpets were formed by such nanobelts through twisting and rolling, respectively. Intriguingly, the nanotwists showed supramolecular chirality with relatively strong CPL performance ($g_{lum} = \pm$ 2.1 $\times$ 10^{-2}) although the component compound is achiral, while the other nanostructure could not.

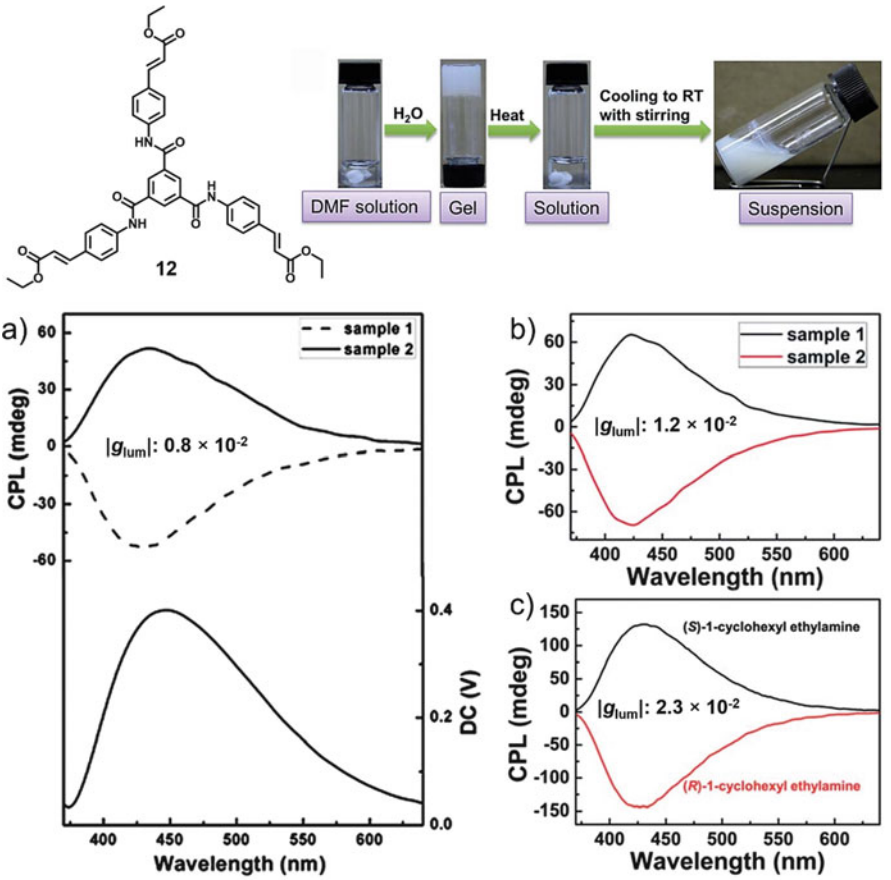

Fig. 11.12 Chemical structure of **12** and photographs showing **12** assemblies in *N,N*-dimethylformamide/H_2O (DMF/H_2O) upon stirring during preparation of the gels (top). (**a**) CPL spectra (left axis) and fluorescence spectra (right axis) of **12** gels in DMF/H_2O. CPL spectra of **12** assemblies after 900 rpm clockwise stirring during gelation (**b**) and containing 900 mol% chiral 1-cyclohexyl ethylamine (**c**) in DMF/H_2O. Reproduced with permission [34]. Copyright 2015, The Royal Society of Chemistry

11.3.3.2 CPL from Chiral Gelator and Achiral Luminophores

As stated above, exclusive achiral luminescent gelators could exhibit CPL through self-assembly in asymmetric environment. In addition, another important approach for the fabrication of CPL-active materials from achiral luminophores is the co-assembly. The chirality transfer from chiral components to achiral luminophores causing induced chirality is of utmost importance. It is not only having potential to endow almost all luminophores with CPL, but also simplify the strategy to produce various CPL-active materials instead of the tedious organic synthesis.

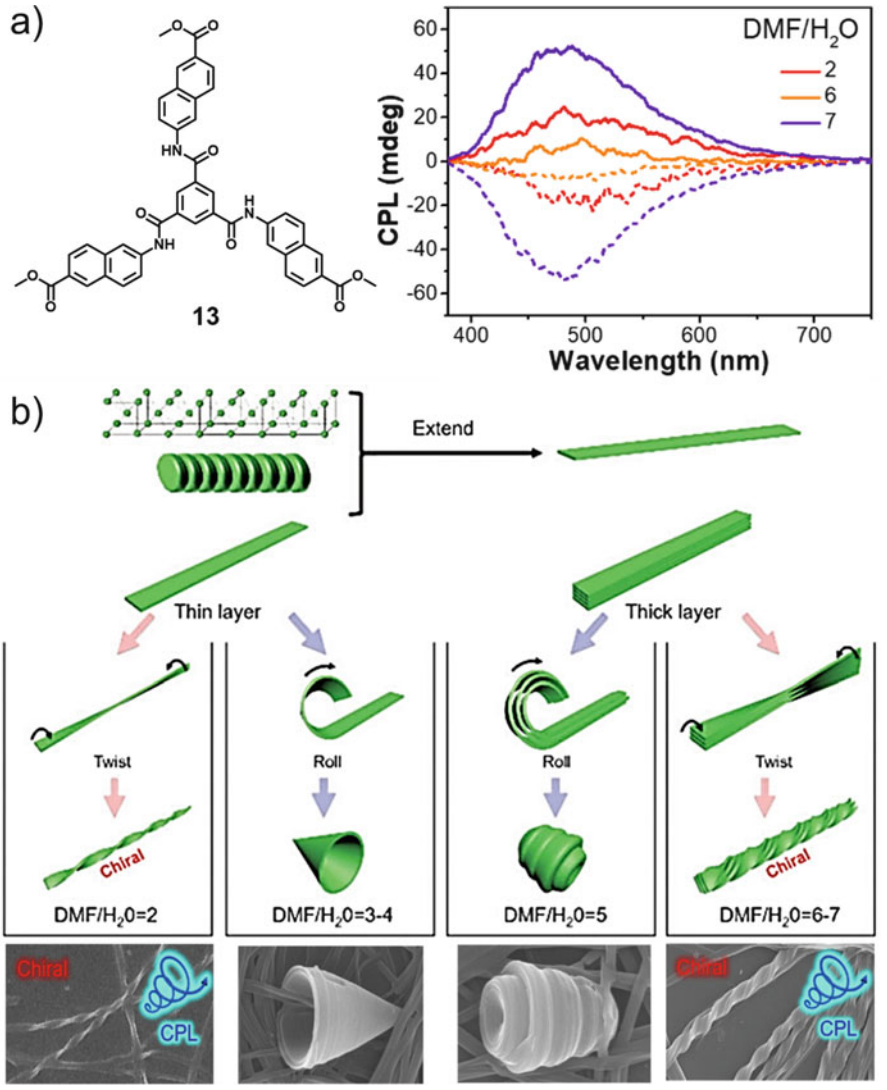

Fig. 11.13 (**a**) Molecular structure for the gelator **13** and CPL spectra of **13** at a volume ratio of DMF/H_2O = 2, 6, and 7. (**b**) Schematics of the formation of nanotwists and nanotrumpets from nanobelts. Bottom was the SEM of the nanotwists and nanotrumpets. The nanotwists showed CPL activities, while the nanotrumpets did not. Reproduced with permission [35]. Copyright 2018, The Royal Society of Chemistry

For the chirality induction of the achiral luminophores, the interaction between the chiral molecules and the achiral luminophores plays a very important role. Noncovalent interactions, such as electrostatic interactions, hydrophobic interactions, hydrogen bonds, and host–guest interactions, could be employed to regulate the chirality induction.

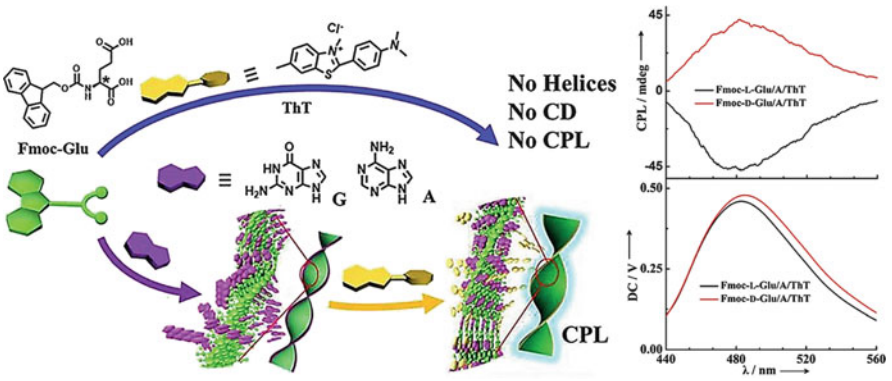

Fig. 11.14 Left: Schematic illustration of the achiral nucleobase-assisted helical self-assembly based on the Fmoc-Glu and supramolecular chirality transfer from Fmoc-Glu to achiral ThT. Right: CPL spectra of Fmoc-(*L*/*D*)-Glu/A/ThT. Reproduced with permission [36]. Copyright 2016, Wiley-VCH

An example of a three-component co-assembly for induced CPL is shown in Fig. 11.14 [36]. Interestingly, the helix of Fmoc-Glu assembly could be triggered by the achiral nucleobase (guanine (G) or adenine (A)). Furthermore, this supramolecular chirality transferred to the achiral cationic dye ThT. It should be noted that only the second achiral molecule is introduced; the co-assembly of Fmoc-Glu and ThT exhibits helicity at the nanoscale level, finally leading to a distinct CPL.

On the other hand, chiral confined spaces or environments can also endow achiral components with chirality. Figure 11.15 shows a general approach to fabricate CPL-active assembly nanotubes through loading achiral AIE luminophores (AIEgens) [37]. As illustrated in Fig. 11.15a, the hexagonal nanotube structures can be constructed by C_3 symmetric chiral gelators *L-/D-***14**, and the intrinsic chirality of the substituted glutamate moieties can transfer to the supramolecular nanotubes during the self-assembly process. Furthermore, the achiral AIE luminophores could be embedded into the confined nanotubes via co-assembly, and achiral AIE dyes aggregated during the gelation process, which showed enhanced fluorescence intensity (Fig. 11.15b) and distinct circularly polarized luminescence by direct excitation. Meantime, the polarization of the CPL is regulated by the supramolecular chirality of the nanotubes. As shown in Fig. 11.15c, through simply altering the doped dyes, mirror-imaged CPL signals from 425 to 595 nm, covering the full-color from blue via green and yellow to orange-red color, can be tuned.

A proton-triggered CPL switch in a co-assembled gel system consisted of a chiral gelator and an achiral fluorophore was showed in Fig. 11.16 [38]. A co-gel could be formed by chiral gelator *L-/D-***15** and achiral perylene bisimide (PBI) in ethanol and gelation-induced chirality of PBI was transferred from *L-/D-***15**. Due to low luminescence efficiency of PBI, no CPL signal could be observed. However, after exposing the co-gel to an acid atmosphere, significantly increased emission intensity

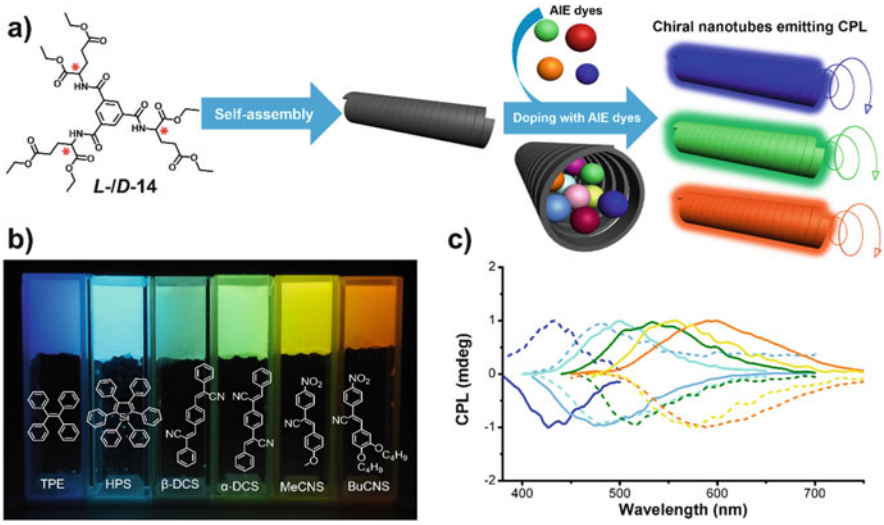

Fig. 11.15 (**a**) Schematic representation of chiral nanotubes formed by *L-/D*-**14** encapsulated different AIE luminophores. (**b**) The photograph of AIEgens-loaded co-gels under UV light irradiation. (**c**) Mirror image CPL spectra of TPE (λ_{ex} = 300 nm), HPS (λ_{ex} = 365 nm), β-DCS (λ_{ex} = 354 nm), α-DCS (λ_{ex} = 363 nm), MeCNS (λ_{ex} = 376 nm), BuCNS (λ_{ex} = 376 nm) in *L*-**14** (solid lines) or *D*-**14** (dash lines) host gels; all the co-gel samples were made in DMSO/H_2O (1/1, v/v) mixing solvents. Reproduced with permission [37]. Copyright 2017, Wiley-VCH

as well as a CPL signal could be detected in the co-gel. Additionally, if the co-gel was exposed to an ammonia atmosphere, both fluorescence and CPL could be switched off. Therefore, this co-gel system achieved a dual switch of fluorescence and CPL (Fig. 11.16a). Because of protonation by acetic acid, the co-gel showed strong fluorescence when under excitation at 447 nm. Meanwhile, CPL was also detected, as verified by the mirror image CPL spectra in Fig. 11.16b. As shown in Fig. 11.16c, when the *L*-15/PBI film was exposed to HCl atmosphere, appearing the fluorescence and CPL curve. However, if exposing the film to an ammonia atmosphere, the fluorescence and CPL will be wiped out. The g_{lum} value showed stable repeatability after several cycle treatments. Therefore, a chiroptical switch based on acid–base exposure regulated could be fabricated.

In the co-assembly system, gelator with photochromic properties could also construct the CPL switch. As illustrated in Fig. 11.17, a photo-switched nanostructure, formed by photosensitive cinnamic acid derivatives (*L*- or *D*-**16**) through self-assembly, can successfully change from superhelix to nanokebab by light irradiation, resulting from the dimerization of cinnamic acid. Meanwhile, the supramolecular chirality could be reversed [39]. Furthermore, fluorescent achiral dyes (CBS) could embed into these helical nanostructures and induced chirality was observed as well as CPL properties. These nanohelixes could turn into nanokebabs by irradiated with UV light (365 nm), and both the inversion of helicity and CPL were observed. Interestingly, the handedness of CPL showed that following the supramolecular chirality of the nanoassemblies rather than the intrinsic molecular chirality. Based

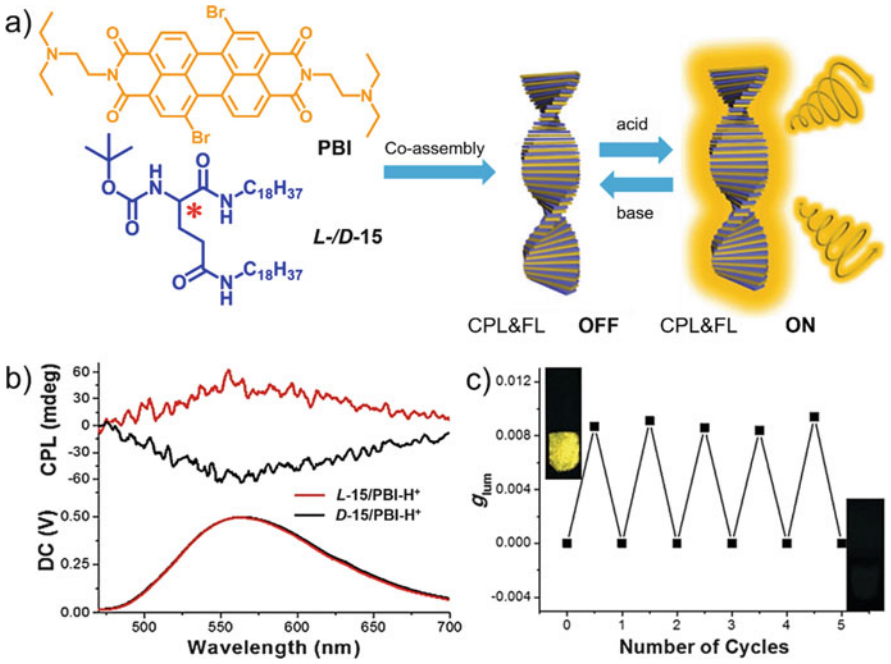

Fig. 11.16 (**a**) Molecular structures of *L-/D-***15** and PBI and schematic illustration of the fabrication of co-gel composed of *L-/D-***15** and achiral PBI. Circularly polarized light emission could be switched by changing acid–base exposure. (**b**) CPL spectra of protonated co-gels (*L*-**15**/PBI and *D*-**15**/PBI) excited at 447 nm. (**c**) Intensity of the CPL g_{lum} value of the co-gel *L*-**15**/PBI against the repeated acid–base exposure cycles. The inset pictures are the gel on quartz under a UV lamp. Reproduced with permission [38]. Copyright 2018, the Royal Society of Chemistry

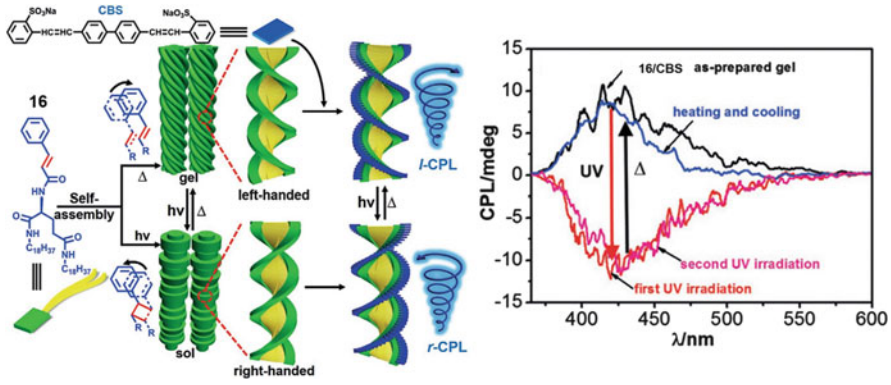

Fig. 11.17 Left: Schematic illustration of the self-assembly nanohelices formed by **16** and co-assembly of **16** with a chiral fluorescent molecule (CBS). The chirality, morphology of formed nanostructures, and induced CPL inversion are triggered by alternating UV irradiation and heating/cooling. Right: CPL spectra of **16**/CBS methanol co-gel under repeated treatment of UV irradiation and heating/cooling. Reproduced with permission [39]. Copyright 2019, Wiley-VCH

on these results, alternative photoirradiation and heating/cooling procedures were utilized to treat the supramolecular nanoassemblies; thus, the inverted helicity and CPL performances could be reversibly repeated during the treatment processes. Therefore, the switched inversion of supramolecular chirality and CPL are successfully realized in one kind of chiral nanostructures by using the co-assembly strategy.

11.4 Conclusion

CPL-active materials have potential applications in various research fields. To achieve this goal, molecular gelator could be regarded as one of the better candidates because of the precisely adjustable intermolecular interactions and enhanced performances in relating to CPL [40–41]. Now, the introduction of new fluorescent materials and the concept of self-assembly have led to the rapid development of CPL-active materials [42–44]. For the research of materials with CPL activities, supramolecular gels provide a broad platform. Besides the self-assembly from chiral luminophores, chiral supramolecular gels could be fabricated from many of the building blocks either chiral or achiral. On the basis of various noncovalent interactions such as H-bond, π–π stacking, host–guest interaction and so on, non-CPL-active isolated chiral gelators could assembly into supramolecular gels exhibiting CPL performance. Analogously, chiral gel matrixes can load or encapsulate achiral luminophores; the achiral luminophores thereby are endowed with CPL activity. This is beneficial not only for organic system but also for inorganic system. Except for the construction of CPL-active materials through gelation, supramolecular gels also can further develop their functions such as energy transfer, CPL switch, and so on. The energy-transfer amplified dissymmetry in gel systems will serve as an excellent platform for expanding the fabrication of highly efficient CPL-active materials. It is worth further research in the future. Although CPL-active gels have shown their application in some cases, a future effort for the CPL application is still in its infancy.

References

1. Josse P, Favereau L, Shen C, Dabos-Seignon S, Blanchard P, Cabanetos C, Crassous J (2017) Enantiopure versus racemic naphthalimide end-capped helicenic non-fullerene electron acceptors: impact on organic photovoltaics performance. Chem Eur J 23:6277–6281
2. Li M, Li SH, Zhang DD, Cai MH, Duan L, Fung MK, Chen CF (2018) Stable enantiomers displaying thermally activated delayed fluorescence: efficient OLEDs with circularly polarized electroluminescence. Angew Chem Int Ed 57:2889–2893
3. Hellou N, Srebro-Hooper M, Favereau L, Zinna F, Caytan E, Toupet L, Dorcet V, Jean M, Vanthuyne N, Williams JAG, Di Bari L, Autschbach J, Crassous J (2017) Enantiopure cycloiridiated complexes bearing a pentahelicenic N-heterocyclic carbene and displaying long-lived circularly polarized phosphorescence. Angew Chem Int Ed 56:8236–8239

4. Schadt M (1997) Liquid crystal materials and liquid crystal displays. Annu Rev Mater Sci 27:305–379
5. Zheng H, Li W, Li W, Wang X, Tang Z, Zhang SX-A, Xu Y (2018) Uncovering the circular polarization potential of chiral photonic cellulose films for photonic applications. Adv Mater 30:1705948
6. Song F, Wei G, Jiang X, Li F, Zhu C, Cheng Y (2013) Chiral sensing for induced circularly polarized luminescence using an Eu(III)-containing polymer and D- or L-proline. Chem Commun 49:5772–5774
7. Yang Y, da Costa RC, Fuchter MJ, Campbell AJ (2013) Circularly polarized light detection by a chiral organic semiconductor transistor. Nat Photonics 7:634
8. Shuvaev S, Suturina EA, Mason K, Parker D (2018) Chiral probes for α1-AGP reporting by species-specific induced circularly polarised luminescence. Chem Sci 9:2996–3003
9. Wang L, Yin L, Zhang W, Zhu X, Fujiki M (2017) Circularly polarized light with sense and wavelengths to regulate azobenzene supramolecular chirality in optofluidic medium. J Am Chem Soc 139:13218–13226
10. Kawasaki T, Sato M, Ishiguro S, Saito T, Morishita Y, Sato I, Nishino H, Inoue Y, Soai K (2005) Enantioselective synthesis of near enantiopure compound by asymmetric autocatalysis triggered by asymmetric photolysis with circularly polarized light. J Am Chem Soc 127:3274–3275
11. Richardson RD, Baud MGJ, Weston CE, Rzepa HS, Kuimova MK, Fuchter MJ (2015) Dual wavelength asymmetric photochemical synthesis with circularly polarized light. Chem Sci 6:3853–3862
12. Yeom J, Yeom B, Chan H, Smith KW, Dominguez-Medina S, Bahng Joong H, Zhao G, Chang W-S, Chang S-J, Chuvilin A, Melnikau D, Rogach AL, Zhang P, Link S, Král P, Kotov NA (2014) Chiral templating of self-assembling nanostructures by circularly polarized light. Nat Mater 14:66
13. He C, Yang G, Kuai Y, Shan S, Yang L, Hu J, Zhang D, Zhang Q, Zou G (2018) Dissymmetry enhancement in enantioselective synthesis of helical polydiacetylene by application of superchiral light. Nat Commun 9:5117
14. Sanchez-Carnerero EM, Agarrabeitia AR, Moreno F, Maroto BL, Muller G, Ortiz MJ, de la Moya S (2015) Circularly polarized luminescence from simple organic molecules. Chem Eur J 21:13488–13500
15. Kumar J, Nakashima T, Tsumatori H, Kawai T (2014) Circularly polarized luminescence in chiral aggregates: dependence of morphology on luminescence dissymmetry. J Phys Chem Lett 5:316–321
16. Dhbaibi K, Favereau L, Srebro-Hooper M, Jean M, Vanthuyne N, Zinna F, Jamoussi B, Di Bari L, Autschbach J, Crassous J (2018) Exciton coupling in diketopyrrolopyrrole-helicene derivatives leads to red and near-infrared circularly polarized luminescence. Chem Sci 9:735–742
17. Gon M, Morisaki Y, Chujo Y (2017) Optically active phenylethene dimers based on planar chiral tetrasubstituted [2.2]paracyclophane. Chem Eur J 23:6323–6329
18. Duan P, Cao H, Zhang L, Liu M (2014) Gelation induced supramolecular chirality: chirality transfer, amplification and application. Soft Matter 10:5428–5448
19. Liu M, Ouyang G, Niu D, Sang Y (2018) Supramolecular gelatons: towards the design of molecular gels. Org Chem Front 5:2885–2900
20. Sheng Y, Ma J, Liu S, Wang Y, Zhu C, Cheng Y (2016) Strong and reversible circularly polarized luminescence emission of a chiral 1,8-naphthalimide fluorophore induced by excimer emission and orderly aggregation. Chem Eur J 22:9519–9522
21. Kumar J, Nakashima T, Kawai T (2015) Circularly polarized luminescence in chiral molecules and supramolecular assemblies. J Phys Chem Lett 6:3445–3452
22. Jintoku H, Kao M-T, Del Guerzo A, Yoshigashima Y, Masunaga T, Takafuji M, Ihara H (2015) Tunable stokes shift and circularly polarized luminescence by supramolecular gel. J Mater Chem C 3:5970–5975

23. Yang D, Duan P, Liu M (2018) Dual upconverted and downconverted circularly polarized luminescence in donor–acceptor assemblies. Angew Chem Int Ed 130:9501–9505
24. Niu D, Ji L, Ouyang G, Liu M (2018) Achiral non-fluorescent molecule assisted enhancement of circularly polarized luminescence in naphthalene substituted histidine organogels. Chem Commun 54:1137–1140
25. Liu J, Su H, Meng L, Zhao Y, Deng C, Ng JCY, Lu P, Faisal M, Lam JWY, Huang X, Wu H, Wong KS, Tang BZ (2012) What makes efficient circularly polarised luminescence in the condensed phase: aggregation-induced circular dichroism and light emission. Chem Sci 3:2737–2747
26. Li HK, Xue S, Su HM, Shen B, Cheng ZH, Lam JWY, Wong KS, Wu HK, Li BS, Tang BZ (2016) Click synthesis, aggregation-induced emission and chirality, circularly polarized luminescence, and helical self-assembly of a Leucine-containing silole. Small 12:6593–6601
27. Yang D, Duan P, Zhang L, Liu M (2017) Chirality and energy transfer amplified circularly polarized luminescence in composite nanohelix. Nat Commun 8:15727
28. Ji L, Sang Y, Ouyang G, Yang D, Duan P, Jiang Y, Liu M (2019) Cooperative chirality and sequential energy transfer in a supramolecular light-harvesting nanotube. Angew Chem Int Ed 58:844–848
29. Bene L, Bagdány M, Damjanovich L (2018) Checkpoint for helicity conservation in fluorescence at the nanoscale: energy and helicity transfer (hFRET) from a rotating donor dipole. Biophys Chem 239:38–53
30. Ajayaghosh A, Praveen VK, Srinivasan S, Varghese R (2007) Quadrupolar π-gels: sol–gel tunable red–green–blue emission in donor–acceptor-type oligo(p-phenylenevinylene)s. Adv Mater 19:411–415
31. Gopal A, Hifsudheen M, Furumi S, Takeuchi M, Ajayaghosh A (2012) Thermally assisted photonic inversion of supramolecular handedness. Angew Chem Int Ed 51:10505–10509
32. Sang Y, Yang D, Duan P, Liu M (2019) Towards homochiral supramolecular entities from achiral molecules by vortex mixing-accompanied self-assembly. Chem Sci 10:2718–2724
33. Okano K, Taguchi M, Fujiki M, Yamashita T (2011) Circularly polarized luminescence of rhodamine B in a supramolecular chiral medium formed by a vortex flow. Angew Chem Int Ed 50:12474–12477
34. Shen Z, Wang T, Shi L, Tang Z, Liu M (2015) Strong circularly polarized luminescence from the supramolecular gels of an achiral gelator: tunable intensity and handedness. Chem Sci 6:4267–4272
35. Sang YT, Duan PF, Liu MH (2018) Nanotrumpets and circularly polarized luminescent nanotwists hierarchically self-assembled from an achiral C-3-symmetric ester. Chem Commun 54:4025–4028
36. Deng M, Zhang L, Jiang Y, Liu M (2016) Role of achiral nucleobases in multicomponent chiral self-assembly: purine-triggered helix and chirality transfer. Angew Chem Int Ed 55:15062–15066
37. Han J, You J, Li X, Duan P, Liu M (2017) Full-color tunable circularly polarized luminescent nanoassemblies of achiral AIEgens in confined chiral nanotubes. Adv Mater 29:1606503
38. Han DX, Han JL, Huo SW, Qu ZM, Jiao TF, Liu MH, Duan PF (2018) Proton triggered circularly polarized luminescence in orthogonal- and co-assemblies of chiral gelators with achiral perylene bisimide. Chem Commun 54:5630–5633
39. Jiang H, Jiang Y, Han J, Zhang L, Liu M (2019) Helical nanostructures: chirality transfer and a photodriven transformation from superhelix to nanokebab. Angew Chem Int Ed 58:785–790
40. Yang D, Zhao Y, Lv K, Wang X, Zhang W, Zhang L, Liu M (2016) A strategy for tuning achiral main-chain polymers into helical assemblies and chiral memory systems. Soft Matter 12:1170–1175
41. Zhao Y, Abdul Rahim NA, Xia Y, Fujiki M, Song B, Zhang Z, Zhang W, Zhu X (2016) Supramolecular chirality in achiral polyfluorene: chiral gelation, memory of chirality, and chiral sensing property. Macromolecules 49:3214–3221

42. Huo SW, Duan PF, Jiao TF, Peng QM, Liu MH (2017) Self-assembled luminescent quantum dots to generate full-color and white circularly polarized light. Angew Chem Int Ed 56:12174–12178
43. Goto T, Okazaki Y, Ueki M, Kuwahara Y, Takafuji M, Oda R, Ihara H (2017) Induction of strong and tunable circularly polarized luminescence of nonchiral, nonmetal, low-molecular-weight fluorophores using chiral nanotemplates. Angew Chem Int Ed 56:2989–2993
44. Shi Y, Duan P, Huo S, Li Y, Liu M (2018) Endowing perovskite nanocrystals with circularly polarized luminescence. Adv Mater 30:1705011